ELSEVIER

Journal of Power Sources 89 (2000) 190–200

JOURNAL OF POWER SOURCES

www.elsevier.com/locate/jpowsour

Molecular dynamics simulations of cathode/glass interface behavior: effect of orientation on phase transformation, Li migration, and interface relaxation

S.H. Garofalini *, P. Shadwell

Department of Ceramic and Materials Engineering, Rutgers University, 607 Taylor Road, Piscataway, NJ 08854, USA

Received 20 September 1999; accepted 10 February 2000

Abstract

The molecular dynamics (MD) computer simulation technique has been used to study electrolyte/cathode interfaces formed in Li-based thin film oxide solid state ionic devices at the atomistic level. The solid electrolytes are lithium silicate glasses while the cathodes are V_2O_5 or WO_3 crystals. The work presented in this paper will focus on the behavior at the glass/V_2O_5 interface. The MD simulation technique has been successfully used to simulate a variety of silicate glasses and glass surfaces, with results consistent with a variety of experimental data. The simulations of the vanadia crystal reproduce the experimental crystal structures, vibrational frequency, and the appropriate phase transition of V_2O_5 as Li ions enter the crystal. The simulations have also shown that Li transport into the crystal is affected by the orientation of the crystal at the interface as well as by surface roughness. While the crystal oriented with the (001) planes parallel to the crystal/glass interface shows the appropriate phase transition to the δ-LiV_2O_5 phase as Li ions enter the crystal, the work presented here shows that the crystal oriented with the (100) planes parallel to the interface does not transform. The difference is attributed to the effect of interface bonding between the ions in the first crystal layer and those in the glass surface. The simulations show a relaxation occurring in a lithium metasilicate glass electrolyte but not in a lithium disilicate electrolyte. In addition, relaxation at the interface between a roughened glass surface and the crystal creates a distortion in the crystal planes in immediate contact with the glass that creates an induced strain in the crystal.

Keywords: Molecular dynamics; Cathode/glass interface; Li

1. Introduction

Solid state lithium ion batteries have been considered for microbattery applications for several decades [1–6] and new materials are constantly being evaluated [7–14]. While bulk properties of the individual components are fairly well understood, the properties at the different interfaces that are created in these systems are not as well understood. The difficulty in obtaining experimental data of interface structure and behavior at an atomistic level has prompted the application of computational techniques to study these interfaces.

The molecular dynamics (MD) computer simulation technique is one important computational approach to addressing these problems. Classical MD simulations rest on the ability of the assumed interatomic potential, from which the force between atoms is derived, to be reasonably accurate in its description of atomistic behavior. In the simulations performed here, the system consists of lithium silicate electrolyte glasses and vanadia cathodes.

We have performed a large number of simulations of silicate glasses, glass surfaces, crystals, and molecules [15–33].

Using a multibody potential, the simulations generated the structure of the simulated silica glass similar to the experimental structure function [18]. The structure of alkali silicate glasses [24] gave the maximum in the first peak in the pair distribution function (PDF) for Na–O at 2.36 Å,

* Corresponding author. Tel.: +1-732-445-2216; fax: +1-732-445-3258.

E-mail address: shg@rutile.rutgers.edu (S.H. Garofalini).

0378-7753/00/$ - see front matter
PII: S0378-7753(00)00429-8

similar to the extended X-ray absorption fine structure (EXAFS) data [34]. More interestingly, the simulations showed the cause for the need for a two-shell model in the curve-fitting of the EXAFS data. Thus, the simulations reproduced the overall EXAFS curve for Na–O exactly, and showed which pairs caused the first shell in the EXAFS calculations.

Simulations of silica and alkali silicate surfaces matched experimental data, without modifying the potentials to specifically address surface properties. Simulations of dry [19] and wet silica [21] surfaces using this multibody potential resulted in structures that were consistent with experimental data (not only qualitatively, but also quantitatively). Early simulations of alkali silicate glass surfaces showed preferential relaxation of K and Na ions to the outer glass surface, but no such behavior for Li ions [17,35,36], consistent with ion scattering spectroscopy (ISS) studies of such glasses [37]. While these early studies used pair potentials, similar results are observed in current simulations with the multibody potentials.

Simulations of the bulk and the surfaces of α-alumina and γ-alumina [28] were done using multibody potentials which allow for the two possible coordinations of the Al atoms in the alumina crystals (i.e., the Al ions can be either octahedrally coordinated in α-alumina and tetrahedrally and octahedrally coordinated in γ-alumina). The simulation results of the alumina systems are in agreement with experimental X-ray diffraction (XRD) data and molecular static calculations. The surface energy of the Al-terminated (0001) alumina surface was found to be 2.0 J/m^2, consistent with the more recent DFT calculations which put the value at 1.95 J/m^2 [38]. In addition, the simulations show a relaxation of the Al ions in the Al-terminated (0001) surface inwards, similar to the ab initio calculations.

In simulations relevant to thin film batteries, we have simulated both V_2O_5 and WO_3 crystals in contact with lithium silicate glasses using multibody potentials in the MD technique [32,39].

In the more recent simulations of the cathode/glass interface, emphasis has been on the V_2O_5 cathode. Constant pressure simulations of the crystal structure matched XRD patterns and unit cell parameters from the literature, as well as the vibrational spectrum [39]. Charge variation in the V ions caused by the local presence of the Li was incorporated in the simulations [39].

The simulations showed a phase transformation from V_2O_5 to δ-LiV_2O_5 as Li ions enter the crystal, which follows the experimental phase diagram [39]. Interestingly, the interatomic potentials were developed for V_2O_5 and γ-LiV_2O_5, not δ-LiV_2O_5. However, the δ-LiV_2O_5 phase is stable with this multibody potential, providing an indication of its value in these simulations. The phase transformation caused by the presence of the Li ions in the vanadia occurs by a glide of the (001) layers in the ⟨010⟩ direction. This phase transformation was observed for the V_2O_5 crystal oriented with the (001) planes parallel to the glass surface (called the '(001) orientation'), but not when the V_2O_5 was oriented with the (010) planes parallel to the glass surface (called the '(010) orientation') [39]. The transformation was shown to be a lateral shift occurring between the layers of the cathode crystal due to the presence of lithium between those layers (see Fig. 1). Those upper layers that did not have Li ions between them did not show the glide transformation (Fig. 1), but did transform after additional Li ions migrated to those layers [39].

We attribute the lack of transformation of the (010) orientation to the required glide of the (001) layers in the ⟨010⟩ direction, which is physically inhibited when the (010) planes are parallel to the surface (see Fig. 2). However, with the (100) planes parallel to the surface, glide in the ⟨010⟩ direction is not inhibited (see Fig. 2), but would be parallel to the interface. This orientation was studied in recent simulations and the results are presented in this paper.

Results of our simulations of the (100)-oriented crystalline vanadia in contact with the electrolyte glass in order to evaluate the transformation to the δ-LiV_2O_5 phase are

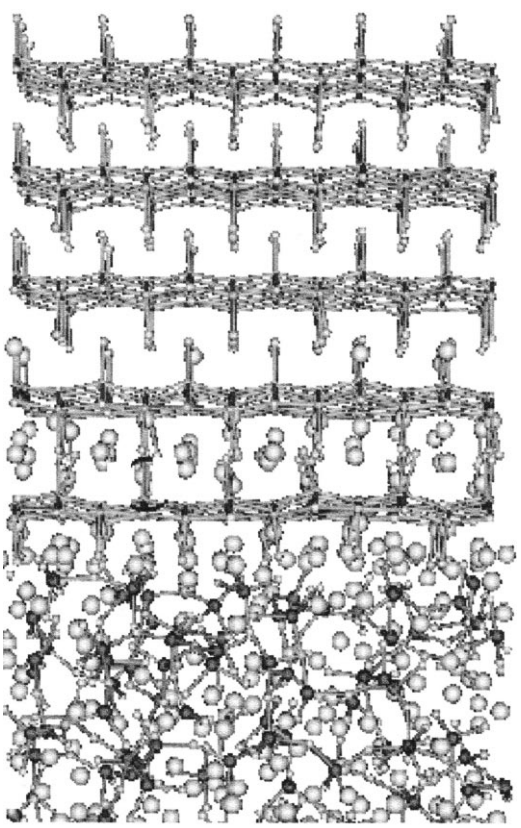

Fig. 1. The (001) planes of vanadia oriented parallel to crystal/glass interface. View is in the ⟨100⟩ direction and shows the shift between layers 1 and 2 caused by the presence of Li ions between the layers. No shift observed in the upper layers.

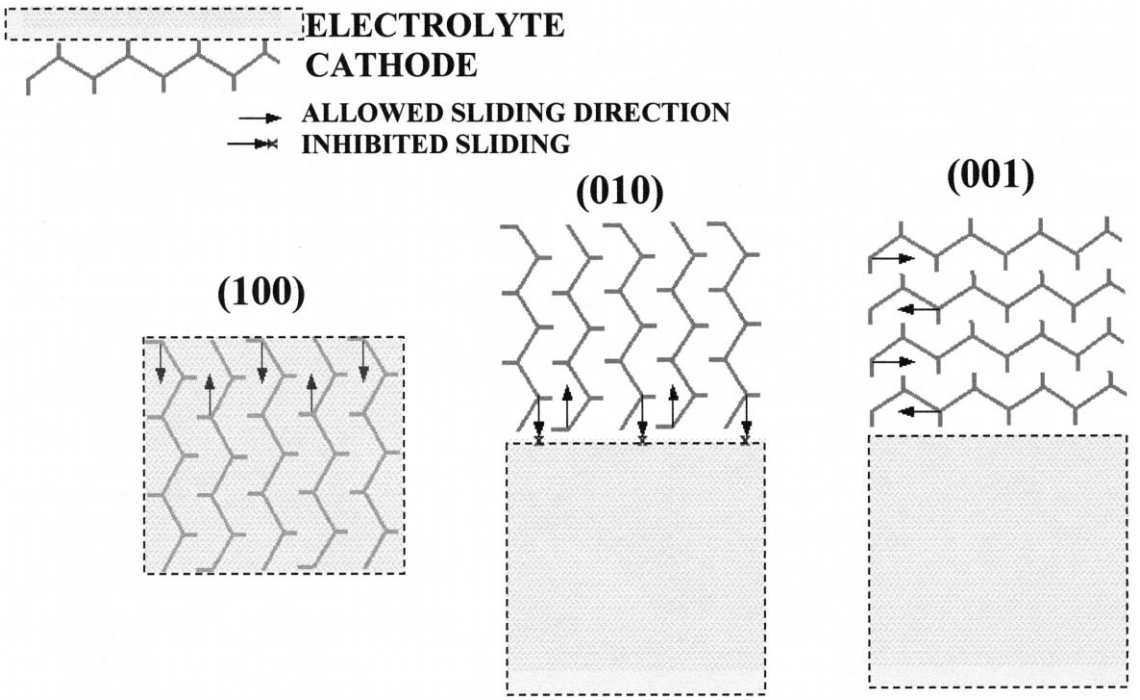

Fig. 2. Three orientations schematically showing ⟨010⟩ glide directions necessary for the phase transformation to the delta lithium vanadate phase.

reported below. In addition, Li buildup at the interface as a function of orientation is also discussed.

2. Computational procedure

2.1. MD technique

The details of the computational procedure have been previously presented [39,40], but important aspects will be briefly reiterated here. The classical MD simulations involve solving Newton's equations of motion for a system of atoms (or ions) interacting via an assumed interatomic potential. The general form of the interatomic multibody potential used here is given as:

$$V(r) = \sum_{i<j} \nu_2(r_i, r_j) + \sum_{i,j,k} \nu_3(r_i, r_j, r_k).$$

The two-body potential (V_2) is given as a modified Born–Mayer–Huggins ionic potential:

$$\nu_2(r_i, r_j) = A_{ij}\exp\left(\frac{-r_{ij}}{\rho_{ij}}\right) + \frac{q_i q_j e^2}{r_{ij}}\xi\left(\frac{r_{ij}}{\beta_{ij}}\right) + V_{ij}^{\mathrm{CSF}},$$

with $r_{ij} = |r_i - r_j|$, q are the charges, ρ_{ij}, A_{ij}, β_{ij} are adjustable parameters, ξ is the complementary error function that acts to reduce the charges as a function of separation distance, and V_{ij}^{CSF} is used to add additional structure to the potential and is given as:

$$V_{ij}^{\mathrm{CSF}} = \sum_{x=1}^{6} \frac{a_{ij}^{x}}{1 + \exp\left(b_{ij}^{x}\left(r_{ij} - c_{ij}^{x}\right)\right)}.$$

V_{ij}^{CSF} is zero for use in the silicates, but was useful in the simulations of vanadia and for systems containing H ions, as described below.

The three-body potential is given as:

$$\upsilon_3(r_i, r_j, r_k) = \phi_{jik}(r_{ij}, r_{ik}, \theta_{jik}) = \lambda_{jik}\exp\left[\gamma_{ij}/\left(r_{ij} - r_i^{\mathrm{c}}\right) + \gamma_{ik}/\left(r_{ik} - r_i^{\mathrm{c}}\right)\right] \times \Omega_{jik}$$

if $r_{ij} < r_i^{\mathrm{c}}$ or $r_{ik} < r_i^{\mathrm{c}}$,

$$= \phi_{jik}(r_{ij}, r_{ik}, \theta_{jik}) = 0 \quad \text{if} \quad r_{ij} > r_i^{\mathrm{c}} \text{ or } r_{ik} > r_i^{\mathrm{c}},$$

β_{ijk}, λ_{ijk}, r^{c}, and $\theta_{jik}^{\mathrm{c}}$ are adjustable parameters and θ_{jik} is the angle between the vectors $\boldsymbol{r}_j - \boldsymbol{r}_i$ and $\boldsymbol{r}_k - \boldsymbol{r}_i$. The three-body contribution Ω_{jik} comes from the atoms i, j, and k, where atoms j and k are covalently bonded to the central atom i. The strength of the three-body term can be varied so as to reflect the covalent nature of the bonds in question (or set to zero if desired). Parameters for the potentials have been previously presented [39].

A fifth-order Nordsieck–Gear predictor–corrector algorithm was used to solve Newton's equation of motion. Both NVE (microcanonical ensemble) and NpT (canonical) simulations were performed. NpT simulations were run using a modified Berendsen algorithm [41] to take into account non-isotropic conditions [28]. Adjustments to the previously published procedure [39,40] were made only in the manner by which surface and interfaces were formed and are presented as needed below.

2.2. Surface and interface formation

The interface between the cathode and electrolyte was formed normal to the z-axis by placing a V_2O_5 crystal surface in contact with a surface of a lithium metasilicate

($Li_2O \cdot Si\ O_2$) glass. System sizes were around 21–25 Å in X and Y (parallel to the surface), with a Z dimension ~ 25 Å for the glass phase and ~ 45 Å for the vanadia phase. Approximately 2800 ions were used and multiple simulations were performed. The sizes varied because of the difference in the orientation of the crystals used in the study. The glass surface farthest from the interface was terminated with frozen atoms and the crystal surface farthest from the interface was terminated with free space in order to simulate a thin film of vanadia on an electrolyte substrate.

Both the (001) and the (100) crystallographic orientations in contact with the glass were simulated. For the (001) orientation, two surface terminations were created: one surface was terminated with vanadium atoms and the other surface was terminated with the oxygen atoms at the end of the vanadyl bond. Both V and O terminations were also used for the (100)-oriented systems. Each termination was made by cleaving the crystal normal to the direction of the appropriate orientation at a position which produced the desired vanadium rich or oxygen-rich surface. The newly cleaved crystal surfaces were not annealed. Fig. 3 shows the crystal terminations for both the (001) and (100) orientations.

The lithium metasilicate, $Li_2O \cdot SiO_2$, glass was made using a constant volume and energy (NVE) melt/quench cycle. The initial simulation box size matched the room temperature X and Y dimensions of the V_2O_5 crystal of the appropriate orientation, but was scaled in accordance with a thermal expansion coefficient of $120.0 \times 10^{-7}°C^{-1}$ at elevated temperatures. The density of the glass at 300 K was 2.323 g/cm.

The periodic boundary condition in the Z dimension of the simulation box was removed to create free glass surfaces perpendicular to the Z axis. Finally, the glass system was put through an annealing cycle in order to relax the newly formed surfaces of broken and strained bonds. The X and Y dimensions for the individual glass and crystal systems were similar to the previous studies, but thicker crystals (larger Z dimension) were used here.

Once the glass and crystal systems had been independently formed, they were joined together in one simulation box to form an 'Interface System'. The X and Y dimensions of the simulation box were kept the same as the crystal simulation box. In the Interface System, the electrolyte glass was annealed one more time to account for the presence of the newly added cathode material above its top surface. During this annealing, the cathode ions were kept immobilized and all glass ions were allowed to move. The relatively short time annealing was done sequentially at the following temperatures and times: 300 K for 0.5 ps, 1000 K for 1 ps, 600 K for 0.5 ps, and 300 K for 0.5 ps. The normal long-time simulations followed annealing.

For the interface simulations, an imaginary plane, called the 'surface plane', was set above the electrolyte surface to mark the point at which lithium ions were considered to have left the glass and entered the interface. For each lithium that crossed this surface plane, a new lithium was added to the bottom of the electrolyte in a volume above the frozen atoms. Adding lithium in this manner main-

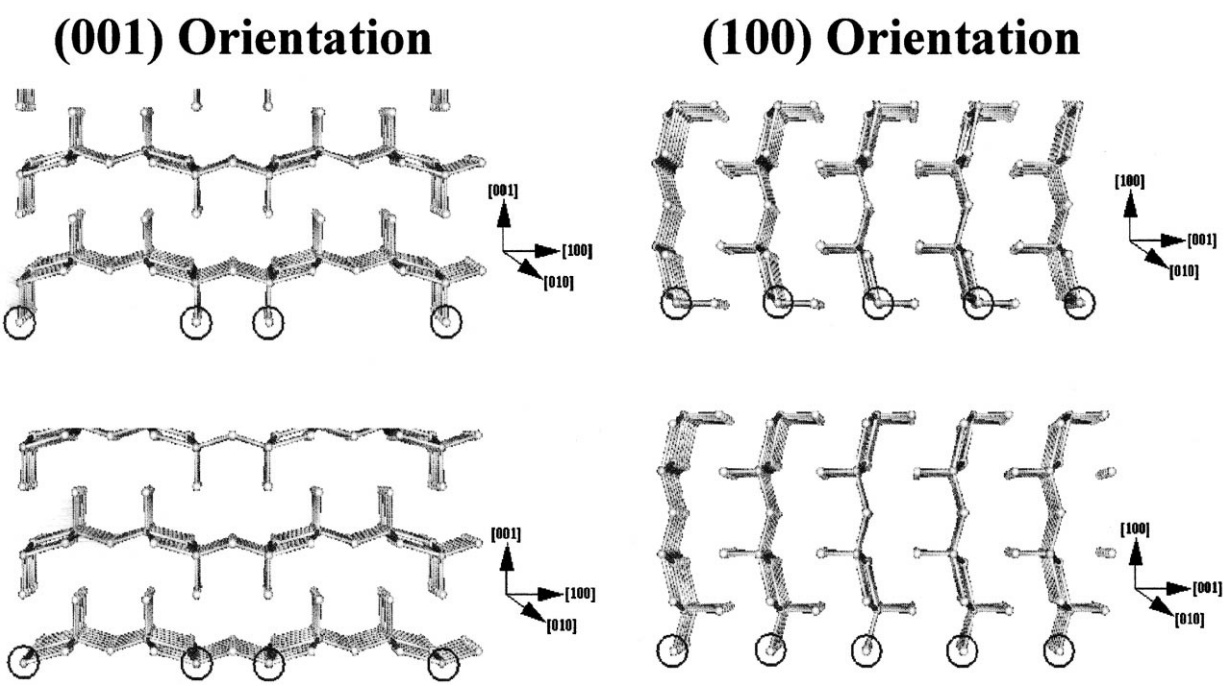

Fig. 3. The O and V terminations of the (100) termination planes.

tained the glass stoichiometry and mimicked a supply of lithium from an imaginary anode.

To find the position of the 'surface plane', a density profile of the electrolyte was generated along the *z*-axis, as shown in Fig. 4. From the plot, the point at which the density of the electrolyte falls to roughly one-half the bulk value — the Gibbs Dividing Surface — was chosen to be the location of the 'surface plane'.

The separation distance between the glass and the crystal was determined by reference to the distance between the 'surface plane' and the bottom layer of the crystal. Separation distances of 2, 3, and 4 Å were used in order to determine the effect of this feature on interface structure and Li intercalation. As a result of this aspect of the work, additional studies were performed in order to address relaxation of the glass surface in the presence of the crystal, as will be presented below.

After the crystal and glass were joined and annealed, simulation runs at 300 K for varying times (from 10 to 100 ps) under NpT conditions were used in order to gather the statistics of interface behavior. All ions except those in the lower frozen region of the glass were allowed to move.

As mentioned above, studying the effect of the initial separation distance between the crystal and the glass when they were first brought together led to an additional study. Specifically, a large glass ($\sim 46 \times \sim 64$ Å^2 in X and Y) was put within 2 Å of a three-layer crystal. The center third of the glass in the largest dimension had glass atoms at the surface removed so that this region was ~ 4–5 Å away from the crystal. Both a lithium metasilicate, $Li_2O \cdot SiO_2$, glass and a lithium disilicate, $Li_2O \cdot 2SiO_2$, glass were used in this study. The metasilicate contains more Li ions and shows considerably less network connectivity (Si−O−Si bond connectivity) than does the disilicate. The effect of this compositional change on smoothing of the glass surface towards the crystal was evaluated. It also provided additional information regarding interface behavior that will be presented below.

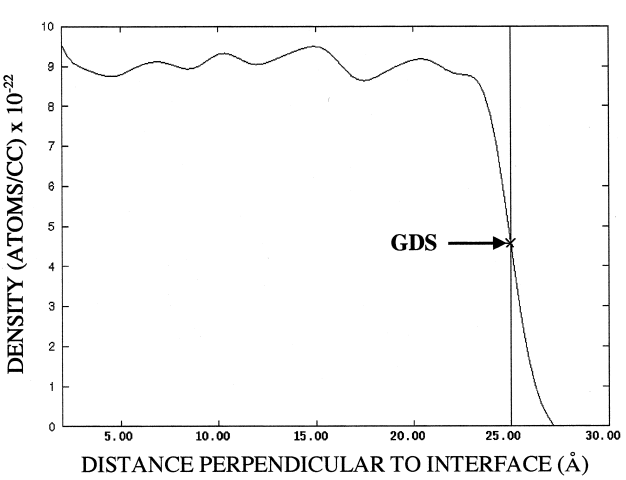

Fig. 4. Density profile of electrolyte glass. The *x* marks values along *z*-axis, which was used to define the 'surface plane'.

3. Results and discussion

3.1. Transformation

At each separation distance, the systems with the electrolyte joined to the (001) surface of the cathode showed that lithium intercalation caused a transformation of the cathode from V_2O_5 to δ-LiV_2O_5. However, the termination location of this orientation, O or V termination, altered the location of the observed transformation.

With the O termination of the (001) orientation, the transformation occurred between the first and second crystalline layers as Li filled the sites between these layers, similar to that shown previously [39,40] and shown in Fig. 5. However, when the cathode in this orientation was terminated with V ions, the transformation was prohibited from occurring between the first and second layers of the cathode and only occurred after Li entered between the second and third crystal layers, as shown is Fig. 5. A better view of this interface is shown in Fig. 6, where the V−O−V bonding between the first and second layers is obvious. This bonding prevents the necessary glide between the first and second layers. The V whose vanadyl oxygen bonds were removed in the first layer are undercoordinated. Combined with the repulsive forces from the Li ions in the glass which quickly move into the interface, these V ions interact with the downward facing vanadyls from the second layer to which they bond. A shortening of the long 'bond' from 2.791 Å to roughly 1.8 Å occurs with a concomitant elongation of the vanadyl bond from the second layer from 1.4 to 1.8 Å. The similarity of these two V−O bonds is shown in Fig. 6 and is similar to a bond in V_2O_3. Once the second crystal layer is bonded to the first crystal layer, the two are restricted from lateral movement and hence, no transformation occurs between these layers, even though Li ions are present.

While we would expect the O-terminated (001) plane to be the more normal situation structurally, the study with the V-terminated surface in contact with the glass provides for an interesting speculation. If some portion of a V_2O_5 crystal shows sufficient interlayer bond formation (for any reason, such as grain boundaries or point defects, or loss of oxygen to locally reduce O concentration, etc., not just that presented here in the simulations), one could expect a change in transformation behavior as well as diffusive behavior of the Li ions. As presented previously [40], Li diffusion in V_2O_5 is very anisotropic. Simulation results showed that the V_2O_5 crystal has a minimum activation barrier of 0.87 eV for Li migration in the ⟨010⟩ direction and a much higher barrier of 2.47 eV for diffusion in the ⟨001⟩ direction. For the δ-LiV_2O_5 phase, a minimum barrier of 0.81 eV in the ⟨010⟩ direction was observed vs. 1.79 eV in the ⟨001⟩ direction [40]. The 'cage' set up by the bonds shown in Fig. 6 would be expected to slow one

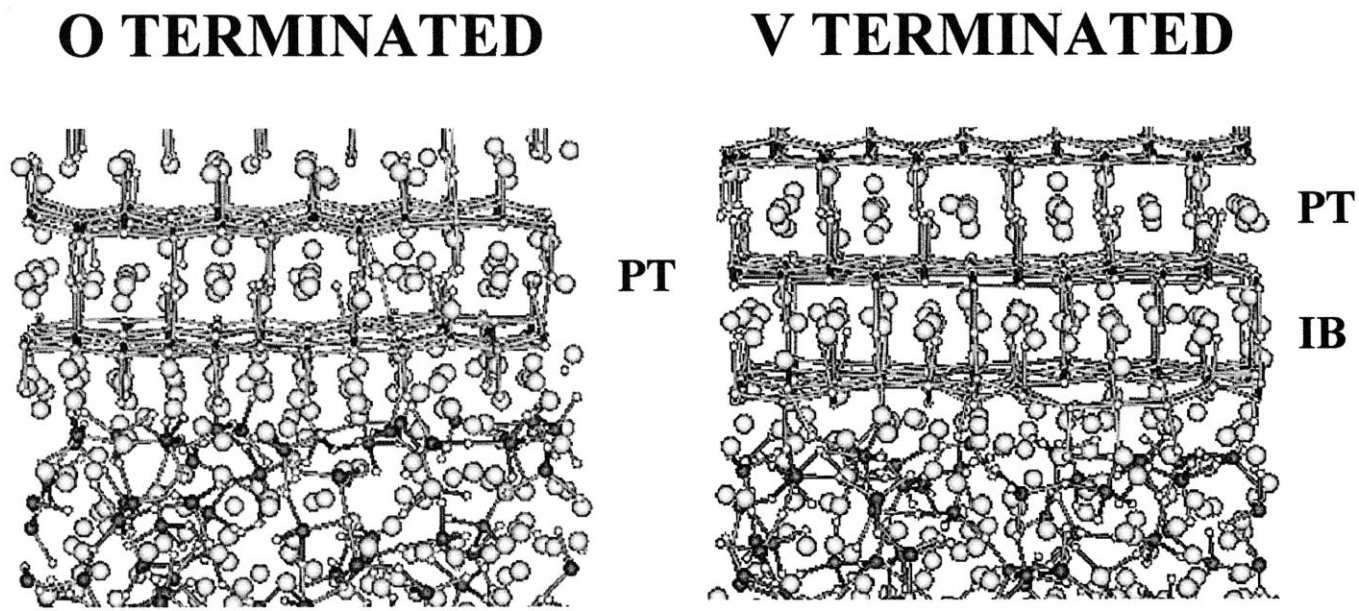

Fig. 5. Phase transformation, labeled PT in the figure, occurs by sliding between layers 1 and 2 in the O-terminated surface, as shown in Fig. 1. In the V-terminated surface, interplanar bonding, labeled IB, prevents the glide between layers 1 and 2 with Li present, but layers 2 and 3 do show the delta phase shift. The IB is shown better in Fig. 6.

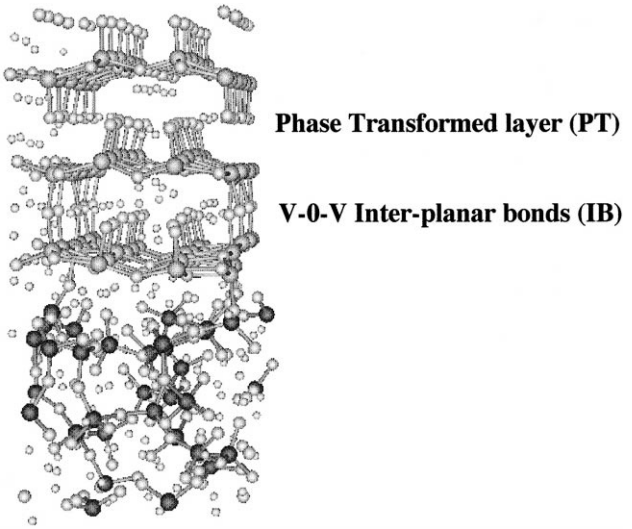

Fig. 6. Slide view of V-terminated (001) interface.

of the more rapid diffusion directions and alter Li transport, perhaps even trapping some Li ions in the crystal during cycling in a manner otherwise unanticipated. This heterogeneity in activation barriers for Li diffusion in vanadia also has some important implications with respect to Li transport across the cathode/glass interface, as presented below.

Although the crystal with the (100) orientation could glide parallel to the crystal/glass interface, as indicated in Fig. 3, the crystal with this orientation did not transform to the delta phase, regardless of the separation distance. This lack of phase transformation is similar to the results for the (010)-oriented crystal [39]. The absence of any transformation in the (100)-oriented system is attributed to interface bonding between the crystal and the glass. Within 20 ps, approximately 20–50% of the crystal ions at the interface bonded to the network ions in the glass. The higher percent of bonding occurred at the smaller initial separation distance, while the lower bonding percent occurred at the larger separation distance. Such bonding inhibits the sliding of the individual crystal layers. So while the crystalline layers in the (100) orientation could slide over the electrolyte surface, as shown schematically in Fig. 3, the bonding between the crystal and the glass prevents this and no transformation is observed.

Such bond formation in the (001) orientation had no affect on the upper (001) planes. Thus, even though bond formation could occur between the first layer of ions in the crystal and the glass surface in the (001)-oriented system, thus anchoring this first layer to the glass, the upper crystalline layers were unaffected by this bonding. Therefore, when sufficient Li ions entered between layers of the (001)-oriented crystal, the upper layer could glide in the ⟨010⟩ direction, affecting the transformation to the δ-LiV_2O_5 phase.

3.2. Interface relaxation

While the different separation distances between the glass and the crystal at the start of the simulation did not have a major effect on the observed phase transformation (or lack thereof in the (100) orientations), there was another interesting result observed in the simulations. The crystal moved slightly inward or outward, depending on orientation and termination. This was anticipated under these constant pressure simulations which had a crystal/vacuum interface away from the glass interface that enabled the crystal to 'float' above the glass and reach some equilibrium spacing with the glass. Of course, this would be affected by the interactions at the crystal/glass interface, such as bonding and Li migration.

More importantly, in addition to the obvious motion of Li ions towards the crystal, the simulations also showed movement of the network ions (Si and O) in the lithium metasilicate glass towards the crystalline layer in the systems with the larger initial separation distance. Since the system is periodic in the *X* and *Y* directions (parallel to the interface), movement of the glass towards the crystal could occur with no restraint laterally. Since the glass was set at a particular initial separation distance, the whole glass surface would experience relatively similar forces at the interface. However, similar simulations using lithium disilicate and lithium trisilicate glasses showed no such relaxation of the network ions in these glasses towards the crystal. The disilicate and trisilicate glasses contain far fewer Li ions than in the metasilicate glass, thus giving glasses with more network connectivity. The greater three-dimensionality of the Si−O connectivity present in the di- and trisilicate glasses creates a less mobile network.

These results raise the interesting question regarding the response of the glassy phase if the glass surface were not uniformly separated from the crystal. That is, what would be the response of the glassy phase if the surface had regions with different separation distances from the crystal? The results would relate to cases where the glass surface is topographically much rougher than the normal atomistic roughness inherent for silica (silicate) glass surfaces [23].

In order to address this question, additional simulations were performed on very large systems containing nearly 10,000 ions. A lithium metasilicate glass was created with a *Y* dimension three times larger than the previous work, an *X* dimension two times larger than the previous work. The crystal/glass separation distance was set at 2.0 Å. However, an additional 2 Å of glass ions in the middle third of the glass in the *Y* dimension was removed from the glass surface, creating a channel in the glass surface, as shown in the schematic below. This created a section of the glass that had a 4.0–4.5 Å separation distance between the glass and the crystal in this portion of the interface. A schematic of the surface of this glass is shown in Fig. 7.

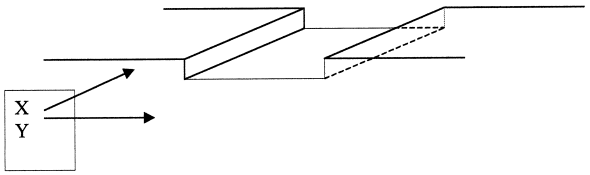

Fig. 7. Schematic drawing of the glass surface with a channel of glass ions removed from the middle third in the *Y* dimension.

Fig. 8a shows a snapshot of the configuration looking from the ⟨100⟩ direction (the horizontal dimension is *Y*). The crystal is in the (001) orientation, with a V termination plane. The sizes of the ions are only for the graphics, with Li ions being the largest spheres in the figure. Si−O and V−O bonds are drawn in the figure. Note the larger separation distance in the middle third of the image in comparison to the outer third, similar to the schematic drawing in Fig. 7. Because of the inherent atomic roughness of the silicate surface, the actual atomistic structure shown in Fig. 8 is not as clean (straight lines) as the schematic in Fig. 7. Fig. 8b shows the interface after 10 ps at 300 K. The ions in the middle third of the glass have moved upward towards the crystal and smoothened the interface considerably in comparison to the initial configuration.

A similar simulation using the lithium disilicate ($Li_2O \cdot 2SiO_2$) glass resulted in little motion of the glass towards filling the crystal/glass gap. The higher network connectivity of the disilicate vs. the metasilicate inhibited the relaxation of the former in comparison to the relaxation

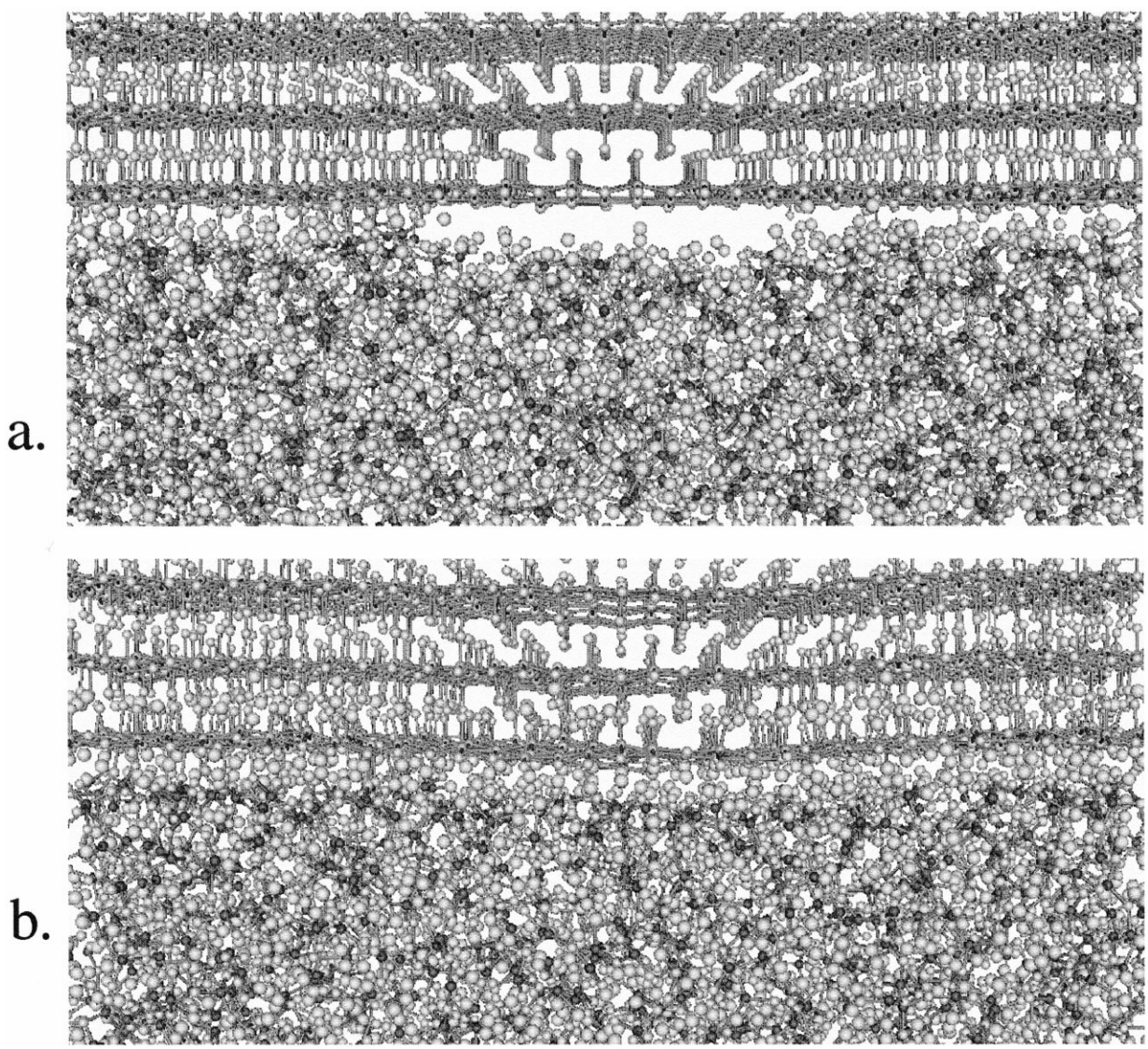

Fig. 8. Lithium metasilicate with three layers of vanadia crystal on top. (a) Starting configuration showing 2 Å separation between the crystal and the glass in the 1st and 3rd of the glass (as measured in the horizontal direction), with additional glass ions removed from the glass surface in the middle third of the glass.

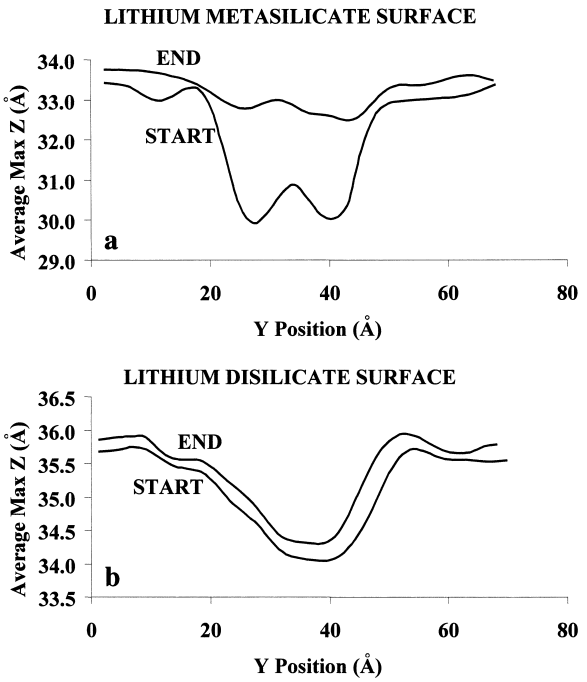

Fig. 9. Relaxation of ions in glass towards crystal in 'channel' structure (see Fig. 7). Maximum Z coordinate of glass ions averaged over X for each Y value. (a) Lithium metasilicate, (b) lithium disilicate. (Note difference in ordinate between a and b.)

that was seen in the metasilicate case. The simulation with the disilicate glass was run for over 100 ps with no additional relaxation of the glass.

Additional representations of the glass surface relaxation behavior are shown in Fig. 9. Here, the highest Z positions of atoms in the glass surface as a function of the atom's Y position, averaged over all X positions at that Y value, are plotted for the initial glass and the final configuration. Clearly, in Fig. 9a, the middle third of the metasilicate glass relaxes upward (towards the crystal which is not shown), while in Fig. 9b, the middle third of the disilicate glass shows little such motion. Because of the greater amount of network connectivity in the disilicate glass than the metasilicate glass, there is a greater restriction in the motion of the silica chains and rings.

Since the outer thirds (first third and third third) of the metasilicate glass is only 2 Å away from the crystal and shows little motion towards the crystal (see Fig. 9a), the connectivity of the middle third to the two outer thirds might be expected to retard relaxation of the middle third towards the crystal. However, the significant amount of Li ions in the metasilicate glass disrupts the network structure so much that short chains and non-bridging oxygen dominate the structure, thus reducing network connectivity. This enables the middle third of the glass to move toward the crystal without the restrictive attachments to the outer thirds.

Also apparent in Fig. 8 of the metasilicate glass is the buildup of Li ions at the crystal/glass interface with this (001) orientation. This buildup was not observed in the simulations with the (010) or (100) orientations. Fig. 10 shows a comparison of this difference in Li behavior at the interface for the (001)- and (010)-oriented interfaces. The

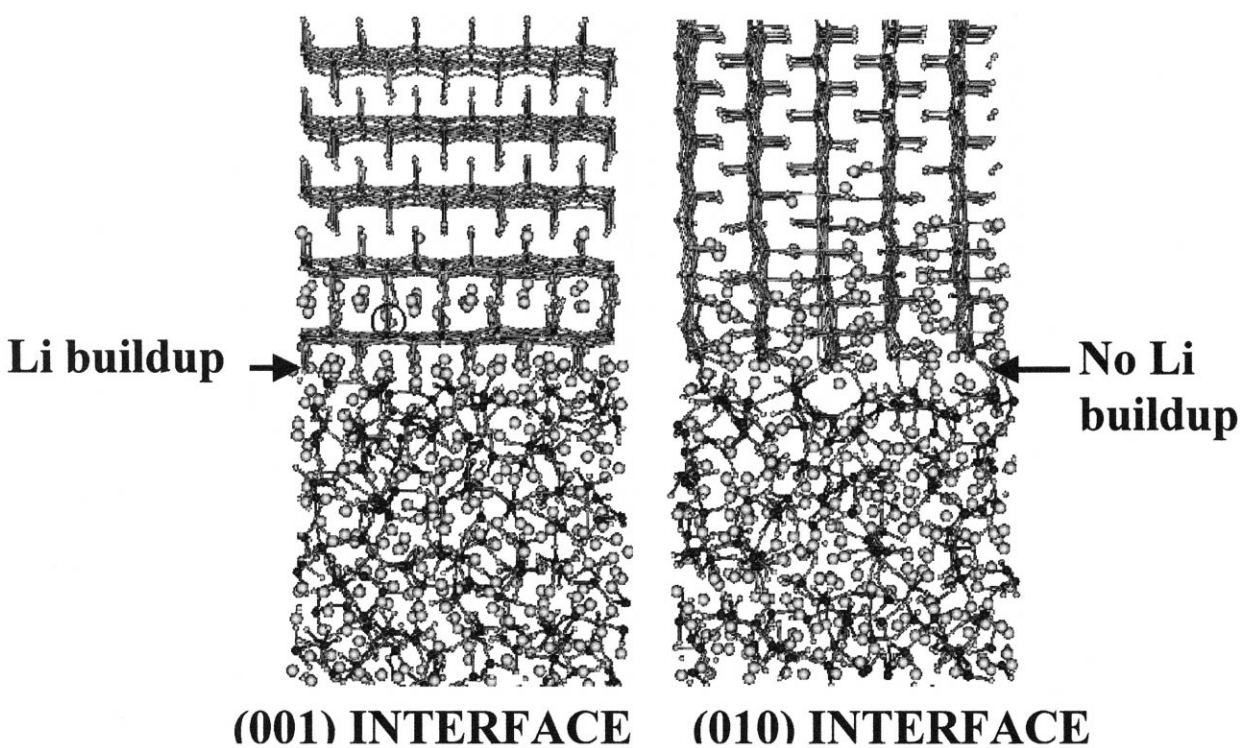

Fig. 10. Li buildup at (001)-oriented interface vs. no buildup in (010) orientation.

buildup of Li ions at the (001) interface can be attributed to the difference in the activation barriers to Li migration in the ⟨001⟩ direction vs. that in the ⟨010⟩ direction. As mentioned above, the barrier in the ⟨001⟩ direction is ~2.5 eV, while the barrier in the ⟨010⟩ direction is only ~0.87 eV [40]. Activation barriers in δ-LiV_2O_5 are similarly anisotropic [40]. The activation energy for Li diffusion in the lithium silicate glasses ranges from 0.78 to 0.85 eV for various lithium silicate glasses. Thus, Li ions diffuse fairly rapidly in the glass towards the vanadia crystal. If the crystal/glass interface has the (001) orientation, there is a much higher activation barrier for Li transport into the crystal in comparison to the barrier in the glass, thus creating a retardation of motion and a buildup of Li ions at the interface. Since the activation barrier for Li transport in the ⟨010⟩ direction is not much different than that for the glass, Li does not build up at the (010)-oriented interface.

Analysis of the interface indicates that there is a Li/V ratio of approximately 1 at the interface in the (001) orientation. Experimental data in the literature have been interpreted by the authors to indicate a buildup of Li ions at the interface region [42]. Their result of 2.82 ($\times 10^{-4}$) C/cm^2 would put the Li concentration at $\sim 1.8 \times 10^{15}$ Li/cm^2. Based on the (001) orientation, with planar unit cell dimensions of 11.51×3.56 $Å^2$, a concentration of 1 Li/2 V in LiV_2O_5 would create a concentration of 0.98×10^{15} Li/cm^2. Thus, their number of $\sim 1.8 \times 10^{15}$ Li/cm^2 is nearly equivalent to 1 Li/V (1.96×10^{15} Li/cm^2), indicating a multilayer adsorption of Li at the interface. Our simulations show Li ions at the interface equivalent to 1 Li/V, similar to the experimental data. In addition, as mentioned previously [39], the simulations showed Li concentrations in the crystal layers with a Li/V ratio near 1.

The simulation results regarding activation barriers for Li transport indicate that if vanadia crystals orient differently with respect to the glass substrate, there will probably be regions with different conductivity behavior.

Finally, Fig. 8 shows an interesting feature regarding the structure of the thin three-layer crystal used in this particular simulation. While in Fig. 8a, the crystalline planes are straight, there is a clear curvature of the planes in Fig. 8b. This effect is shown more clearly in Fig. 11, which is the same structure as in Fig. 8, but only a thin section (into the plane of the figure) is drawn. The crystal layers relax to the shape of the glassy surface in Figs. 11b and 8b, thus creating distorted crystalline planes near the interface. These crystal planes contain strained bonds in the most distorted parts of the plane and could affect the mechanical integrity of the film.

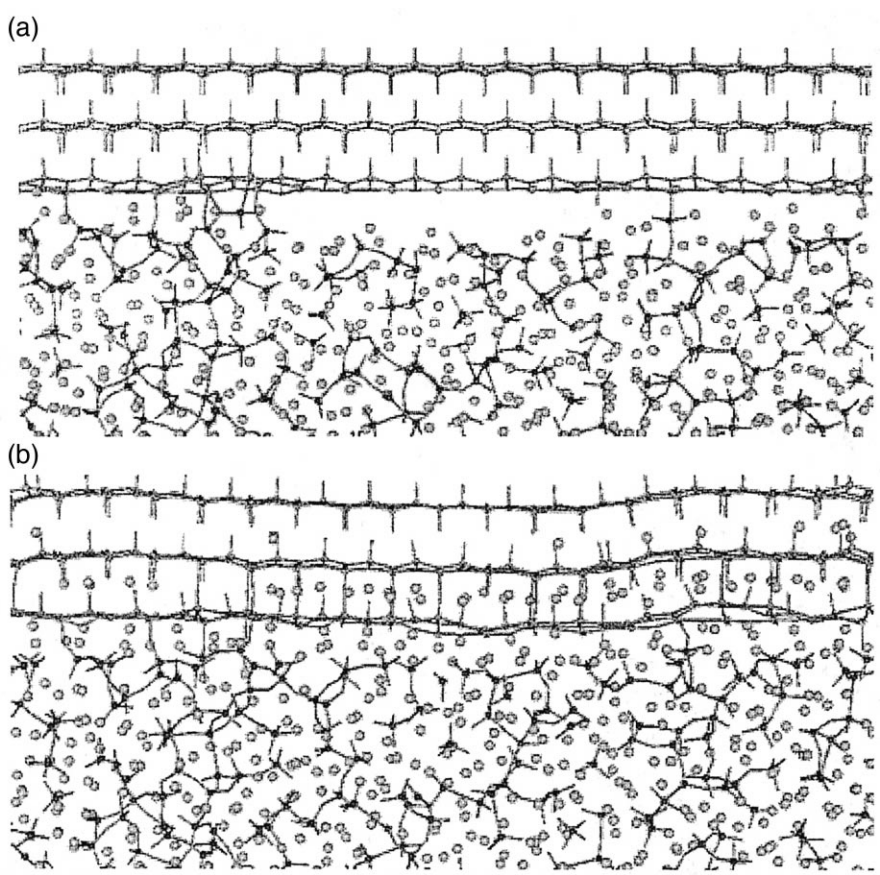

Fig. 11. Similar to Fig. 8, but only a thin section into the plane of the figure shown here. (a) Start of run, (b) end of run, showing curvature of crystal planes.

4. Conclusions

The application of the MD computer simulation technique to studies of thin film lithium ion batteries has shown results which are consistent with the structural features of the cathode crystal and the electrolyte glass films. The phase transformation to the δ-LiV_2o_5 phase as Li ions enter the crystal is affected by interfacial bonding between the crystal and the glass in the (100) orientation, but not the (001) orientation (except at the first crystal layer). The large anisotropy of Li diffusion into the crystal alters migration of Li ions into the crystal, creating a buildup of Li at the interface in the (001) orientation, but no such buildup in the (010) and (100) orientations.

Relaxation of the ions in the metasilicate glass enables a smoothening of rough interfaces, which does not occur as readily in the lithium disilicate glass.

References

[1] M.S. Whittingham, J. Electrochem. Soc. 123 (1976) 315.
[2] M.S. Whittingham, Prog. Solid State Chem. 12 (1978) 1.
[3] B.V.R. Chowdari, S. Radhakrishna, World Scientific Publishing, Singapore, 1988.
[4] K. Kanehori, K. Matsumo, K. Miyauchi, T. Kudo, Solid State Ionics 9/10 (1983) 1445–1448.
[5] K. West, B. Zachau-Christiansen, S.V. Skaarup, F.W. Poulsen, Solid State Ionics 57 (1992) 41–47.
[6] S.D. Jones, J.R. Akridge, F.K. Shokoohi, Solid State Ionics 69 (1994) 357–368.
[7] L. Hernan, J. Morales, L. Sanchez, J. Santos, Solid State Ionics 118 (1999) 179–185.
[8] J. Kawakita, M. Takashi, T. Kishi, Solid State Ionics 120 (1999) 109–116.
[9] S.G. Kang, S.Y. Kang, K.S. Ryu, S.H. Chang, Solid State Ionics 120 (1999) 155–161.
[10] N.J. Dudney et al., J. Electrochem. Soc. 146 (1999) 2455–2464.
[11] J.B. Bates et al., J. Power Sources 43/44 (1993).
[12] J.B. Bates, G.R. Gruzalski, N.J. Dudney, C.F. Luck, X. Yu, Solid State Ionics 70/71 (1994) 619–628.
[13] F.X. Hart, J.B. Bates, J. Appl. Phys. 83 (1998) 7560–7566.
[14] B.J. Neudecker, R.A. Zuhr, J.B. Bates, J. Power Sources 81–82 (1999) 27–32.
[15] S.H. Garofalini, J. Chem. Phys. 76 (1982) 3189–3192.
[16] S.H. Garofalini, J. Chem. Phys. 78 (1983) 2069–2072.
[17] S.H. Garofalini, S. Levine, J. Am. Ceram. Soc. 68 (1985) 376–379.
[18] B.P. Feuston, S.H. Garofalini, J. Chem. Phys. 89 (1988) 5818–5824.
[19] B.F. Feuston, S.H. Garofalini, J. Chem. Phys. 91 (1989) 564–569.
[20] D.M. Zirl, S.H. Garofalini, J. Am. Ceram. Soc. 73 (1990) 2848–2856.
[21] B.P. Feuston, S.H. Garofalini, J. Appl. Phys. 68 (1990) 4830–4836.
[22] B.F. Feuston, S.H. Garofalini, J. Phys. Chem. 94 (1990) 5351–5356.
[23] S.H. Garofalini, J. Non-Cryst. Solids 120 (1990) 1–12.
[24] H. Melman, S.H. Garofalini, J. Non-Cryst. Solids 134 (1991) 107–115.
[25] D.C. Athanasopoulos, S.H. Garofalini, Surf. Sci. 273 (1992) 129–138.
[26] S.H. Garofalini, G. Martin, J. Phys. Chem. 98 (1994) 1311–1316.
[27] E.B. Webb, S.H. Garofalini, Surf. Sci. 319 (1994) 381–393.
[28] S. Blonski, S.H. Garofalini, Surf. Sci. 295 (1993) 263–274.
[29] S. Blonski, S.H. Garofalini, Catal. Lett. 25 (1994) 325–336.
[30] S. Blonski, S.H. Garofalini, J. Phys. Chem. 100 (1996) 2201–2205.
[31] S. Blonski, S.H. Garofalini, J. Am. Ceram. Soc. 80 (1997) 1997–2004.
[32] D. Kulp, S.H. Garofalini, J. Electrochem. Soc. 143 (1996) 2211–2219.
[33] D.A. Litton, S.H. Garofalini, J. Non-Cryst. Solids 217 (1997) 250–263.
[34] G.N. Greaves, A. Fontaine, P. Lagarde, D. Raoux, S.J. Gurman, Nature 293 (1981) 611–616.
[35] S.H. Garofalini, J. Am. Ceram. Soc. 67 (1984) 133–136.
[36] S.H. Garofalini, Phys. Chem. Glass 26 (1985) 166–170.
[37] J. Kelso, C.G. Pantano, S.H. Garofalini, Surf. Sci. 134 (1983) L543–L549.
[38] I.G. Batirev, A. Alavi, M.W. Finnis, T. Deutsch, Phys. Rev. Lett. 82 (1999) 1510–1513.
[39] M. Garcia, E. Webb, S.H. Garofalini, J. Electrochem. Soc. 145 (1998) 2155–2164.
[40] M. Garcia, S.H. Garofalini, J. Electrochem. Soc. 146 (1999) 840–849.
[41] H. Berendsen, J. Postma, W. van Gunsteren, A. DiNola, J. Haak, J. Chem. Phys. 81 (1984) 3670–3684.
[42] J.-S. Bae, S.-I. Pyun, J. Alloys Compd. 217 (1995) 52–58.